IEEE Access
Multidisciplinary | Rapid Review | Open Access Journal

Received 1 February 2024, accepted 11 February 2024, date of publication 23 February 2024, date of current version 4 March 2024.

Digital Object Identifier 10.1109/ACCESS.2024.3369180

RESEARCH ARTICLE

Multilayer Decomposition Denoising Empowered CNN for Radar Signal Modulation Recognition

MENGTING JIANG, FANG ZHOU, LAI SHEN, XIAOFENG WANG, DAYING QUAN, (Member, IEEE), AND NING JIN
School of Information Engineering, China Jiliang University, Hangzhou 310018, China

Corresponding author: Fang Zhou (zhoufang1026@cjlu.edu.cn)

This work was supported in part by the National Natural Science Foundation of China under Grant 62261014, and in part by the Key Research and Development Projects in Zhejiang Province under Grant 2022C01144.

ABSTRACT Radar signal recognition plays a crucial role in modern electronic reconnaissance systems. With the increasing complexity of electromagnetic environments, radar signals are susceptible to noise interference under low signal-to-noise ratio (SNR) conditions, posing a challenge to accurate radar signal recognition. To address this issue, we propose a multilayer decomposition denoising empowered convolutional neural network (CNN) for radar signal recognition. Specifically, the original radar signals are first processed by multilayer decomposition denoising, which consists of variational mode decomposition (VMD), local mean decomposition (LMD), and wavelet thresholding (WT) in sequence, termed as VMD-LMD-WT. Then we use the Choi-Williams distribution (CWD) to convert the denoised signals into time-frequency images (TFIs). Finally, an improved CNN with dilated convolution is employed for radar signal recognition. Experiments demonstrate that the multilayer decomposition denoising method effectively improves the SNR of the original signal, which is beneficial for the subsequent recognition task. The recognition accuracy is improved by about 11% compared to that directly using the original signal. Furthermore, compared to the current network models, the proposed CNN network can efficiently extract the signal features and improve the detection accuracy of low probability of intercept (LPI) radar signals. The recognition accuracy reaches 75.3% for 12 signals when the SNR is low to −14dB.

INDEX TERMS LPI radar signal recognition, signal denoising, time-frequency analysis, convolutional neural network.

I. INTRODUCTION

Radar signal recognition is an essential component of radar electronic reconnaissance and holds significant importance in radar electronic countermeasures [1]. With an increasing number of radar radiation sources, the electromagnetic environment becomes increasingly complex. In practical applications, radar signals captured by the receiver are often disturbed by noise, leading to relatively low signal-to-noise ratios (SNR). This presents a difficulty for radar signal recognition under low SNRs. Feature extraction is of great significance for radar signal recognition. Therefore, there is an urgent need for improvement of the feature extraction, especially in the case of low SNRs.

The associate editor coordinating the review of this manuscript and approving it for publication was Brian Ng.

Traditional methods for radar signal recognition often rely on manual experience and expertise for extraction of conventional parameters and pulse description words (PWD), and then perform relatively simple recognition tasks [2]. However, in complex electromagnetic environments, analyzing features from a single domain is insufficient. In view of this point, time-frequency analysis methods are employed to address the constraints of individual time-based or frequency-based feature extraction, which has become one of the most widely used feature extraction techniques. Techniques that include the Wigner-Ville distribution (WVD) [3], short-time Fourier transform (STFT) [4], and Choi-Williams distribution (CWD) [5] are commonly used to simultaneously characterize signals in the time-frequency domain. Qu et al. [6] extracted the time-frequency images (TFIs) of the incoming signals using a multi-core Cohen-like time-frequency

distribution. Then, a convolutional denoising autoencoder (CDAE) and a deep convolutional neural network (DCNN) were designed to achieve improved classification for twelve signals. In [7], the CWD method was employed to generate TFIs, and the obtained TFIs were served as input to a convolutional neural network in order to identify radar signals. This approach enhanced the robustness against noise and improved the accuracy of recognition. In [8], the authors adopted CWD and WVD to generate TFIs and proposed an approach using single-shot multi-box detector (SSD) and complementary classifier to identify 12 various kinds of radar signals.

As the common adaptive signal decomposition methods, empirical mode decomposition (EMD), local mean decomposition (LMD) [9], and variational modal decomposition (VMD) have found extensive applications in signal denoising analysis, mechanical fault identification, and other fields. Huang et al. [10] introduced EMD to decompose non-smooth signals into multiple eigenmode functions in the time domain. By analyzing the various eigenmodal functions, a certain degree of noise reduction is achieved by the reconstruction with more valuable signal information. Nevertheless, the EMD method lacks rigorous mathematical proof and is subject to end-point effects and modal aliasing. LMD [11] has the ability to decompose signals into the combination of a finite number of single-component amplitude modulation (AM) and frequency modulation (FM) signals, obtaining the product function (PF) components with clear physical meaning. However, the LMD technique still exhibits endpoint effects. Taking this into account, Dragomiretskiy et al. introduced VMD, a novel adaptive time-frequency analysis technique [12]. Compared with EMD and LMD, VMD overcomes the problems of endpoint effects and modal aliasing and has other outstanding advantages in dealing with non-smooth signals and noise suppression. Recently, numerous enhanced VMD methods have been proposed, including sequential variational mode decomposition (SVMD) [13], [14] and multivariate variational modal decomposition (MVMD) [15]. By combining VMD and slope entropy (SloE), a new feature extraction method is presented to obtain high recognition accuracy of ship-radiated noise signals [16]. In [17], Jiang et al. proposed a denoising method based on VMD and Hilbert transform to enhance the accuracy of leak localization in water pipeline systems. This method selectively chose components with energy amplitudes greater than half of the maximum energy amplitude for reconstruction. However, it's worth noting that these VMD-based signal analysis methods directly eliminate parts of the IMF [18], potentially leading to the loss of valuable information embedded in these IMF components.

In order to make full use of the useful information in uncorrelated IMFs, we propose a multilayer decomposition denoising empowered CNN approach for low probability of intercept (LPI) radar signal recognition in this paper. The denoising scheme combines VMD, LMD, and wavelet thresholding (termed as VMD-LMD-WT). Figure 1 depicts the overall structure of the approach. We first employ the VMD-LMD-WT method to denoise the time-domain signals and subsequently analyze the denoised signals using the CWD to obtain TFIs. After preprocessing, the denoised TFIs are input into an improved CNN for deep feature extraction and recognition of signal modulation types. In the CNN, we use dilated convolution instead of normal convolution to increase the receptive field without sacrificing the feature map size. Finally, the aforementioned CNN model is used for classification which successfully recognizes 12 types of LPI radar signals.

II. SIGNAL MODEL AND BASIC THEORY

A. SIGNAL MODEL

The received radar signal is generally contaminated by noise, expressed as:

$$y(t) = x(t) + n(t) = A\exp(j2\pi f_k(t) + \varphi_k) + n(t) \quad (1)$$

where $x(t)$ denotes the observed radar signal, $n(t)$ represents the additive white complex Gaussian noise (AWGN), and A is the amplitude. $f_k(t)$ and φ_k are respectively the carrier frequency and phase functions, which determine the modulation of the radar signal.

This paper verifies the performance of the proposed method by detecting 12 typical LPI modulation types. The modulation types include FM signals (LFM, Costas), BPSK, polyphase codes (Frank, P1, P2, P3, P4), and multi-temporal codes (T1, T2, T3, T4).

B. VARIATIONAL MODE DECOMPOSITION

The basic idea of VMD [19], [20], [21] is to use an iterative method to identify the optimal solution to the variational issue, which can efficiently determine the optimal center frequency and finite bandwidth. The VMD can avoid the inevitable endpoint effect and the problem of modal component mixing in the EMD algorithm. The process of VMD is composed of two stages: constructing the variational model and determining the optimal solution of the variational model. The first stage is to construct a variational model. We first assume that the input signal can be split into k modal components $\{u_k\}$ each of which possesses a specific center frequency and finite bandwidth. The Hilbert transform is then used for the modal component to obtain the analytic signal. Subsequently, the analytic signal is mixed with the predicted center frequency to modulate the spectrum of each modal component to the frequency band. Finally, we calculate the squared L^2 paradigm of the signal gradient. The constrained variational model can be represented as follows:

$$\min_{\{u_k\},\{\omega_k\}} \{\sum_k \left\| \partial_t[\delta(t) + j/\pi t) * u_k(t)]e^{-j\omega_k t} \right\|_2^2\}$$
$$\text{s.t.} \sum_{k=1}^{K} u_k(t) = x(t) \quad (2)$$

where $\{u_k\}$ represents the k-th modal component with the center frequency $\{\omega_k\}$. K indicates the number of modes to

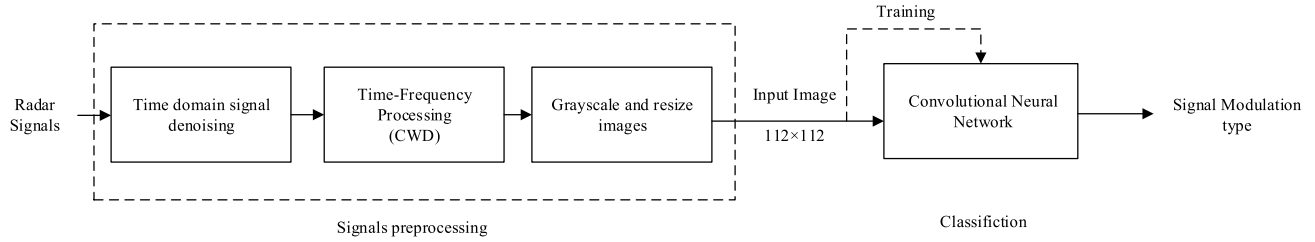

FIGURE 1. The overall framework of LPI radar signal recognition.

be decomposed, $\delta(t)$ denotes the Dirac function, and $*$ is the convolution operator.

Secondly, the optimal solution of the variational model is solved by applying the Lagrange multiplier method which transforms the constrained variational issue into an unconstrained one,

$$\begin{aligned} &L(\{u_k\},\{\omega_k\},\lambda) \\ &= \alpha \sum_k \left\| \partial_t [(\delta(t) + j/\pi t) * u_k(t)] e^{-j\omega_k t} \right\|_2^2 \\ &\quad + \left\| x(t) - \sum_k u_k(t) \right\|_2^2 + \left\langle \lambda(t), x(t) - \sum_k u_k(t) \right\rangle \end{aligned} \tag{3}$$

where $L(\cdot)$ and λ symbolize the Lagrangian function and the Lagrange multiplier, and α is a quadratic penalty factor.

C. LOCAL MEAN DECOMPOSITION

LMD is a signal decomposition method that breaks down a random signal into a limited number of sums of PF components. The PF component is calculated by multiplying the envelope and the pure FM signal [22], [23]. The process combines the instantaneous frequency and amplitude, resulting in full time-frequency distribution of the original signal. The LMD is improved with respect to endpoint effects, spurious components, and over-envelope and under-envelope problems. In the signal decomposition procedure, we first find the neighboring local extremes n_i and n_{i+1} of $x(t)$, and then evaluate the local mean m_i and the local amplitude a_i,

$$m_i = \frac{n_i + n_{i+1}}{2} \tag{4}$$

$$a_i = \frac{|n_i - n_{i+1}|}{2} \tag{5}$$

These local means m_i are extended in a straight line between adjacent extreme points. Then the straight line is smoothed using the sliding average method to form a local mean function $m_{11}(t)$. Similarly, we can derive an envelope estimation function $a_{11}(t)$.The local mean function is then separated from the original signal,

$$h_{11}(t) = x(t) - m_{11}(t) \tag{6}$$

The FM signal $s_{11}(t)$ is obtained by dividing $h_{11}(t)$ by $a_{11}(t)$, expressed as:

$$s_{11}(t) = \frac{h_{11}(t)}{a_{11}(t)} \tag{7}$$

By repeating the above steps, the envelope $a_{12}(t)$ of $s_{11}(t)$ can be obtained. If $a_{12}(t) \neq 1$, continue with the preceding stages until $s_{1n}(t)$ becomes a pure frequency modulated signal. The envelope signal $a_1(t)$ is the product of all envelope estimation functions,

$$a_1(t) = a_{11}(t)a_{12}(t)\cdots a_{1n}(t) = \prod_{q=1}^{n} a_{1q}(t) \tag{8}$$

The $PF_1(t)$ component of the original signal is the product of the envelope signal $a_1(t)$ and the pure FM signal $s_{1n}(t)$,

$$PF_1(t) = a_1(t)s_{1n}(t) \tag{9}$$

$u_1(t)$ is obtained by splitting $PF_1(t)$ component from the initial signal $x(t)$. Repeat (4) through (9) until $u_N(t)$ is a monotone function. Finally, $x(t)$ is split into N PF components and $u_N(t)$,

$$\begin{aligned} u_1(t) &= x(t) - PF_1(t) \\ u_2(t) &= u_1(t) - PF_2(t) \\ &\vdots \\ u_k(t) &= u_{k-1}(t) - PF_k(t) \end{aligned} \tag{10}$$

$$x(t) = \sum_{q=1}^{N} PF_q(t) + u_N(t) \tag{11}$$

III. DENOISING METHOD AND NETWORK MODEL

A. VMD-LMD-WT Denoising Method

Traditional noise reduction techniques using filters can selectively remove noise in a particular frequency band. For instance, noise in the high frequencies can be eliminated by a low-pass filter, while noise in the low frequencies can be eliminated by a high-pass filter. However, this method requires predetermined filter types and parameters. Different from the aforementioned methods, the denoising method based on VMD can potentially remove the noise from the signal components in wide frequency ranges. The VMD divides the input signal into numerous IMFs, with each IMF representing different frequency bands. The low amplitude noise components can be more accurately eliminated on each IMF using thresholding or other denoising methods. In this paper, AWGN is added to the signals, characterized by its spectral density being evenly distributed over the entire spectrum. Therefore, the latter method is more appropriate for signal denoising in this study.

However, VMD denoising requires the manual selection of parameters and IMF components, leading to insufficient noise reduction. To address this problem, we propose a multilayer denoising algorithm based on VMD-LMD-WT. In particular, VMD performs excellently when splitting complex non-stationary signals into a series of IMFs. LMD is good at dealing with these relatively simple IMFs and the resulting PFs have clear physical meaning [24]. Wavelet decomposition is a powerful time-frequency analysis tool, which has found widely application in signal and image processing. Through the integration of these methods, a more precise decomposition of the signal at various frequencies and time scales is obtained. Multi-layer denoising methods provide comprehensive adaptive solutions for signal noise reduction and help to understand the characteristics of the signal. By performing denoising layer by layer, the effect of noise on the signal can be minimized, and the useful information of the signal can be retained. In the proposed algorithm, the signal is divided into two parts: noise-dominated and signal-dominated. Our primary objective is to denoise the noise-dominated part of the signal, extracting a small quantity of useful signals that are hidden by the noise, and avoiding the loss of valuable signals.

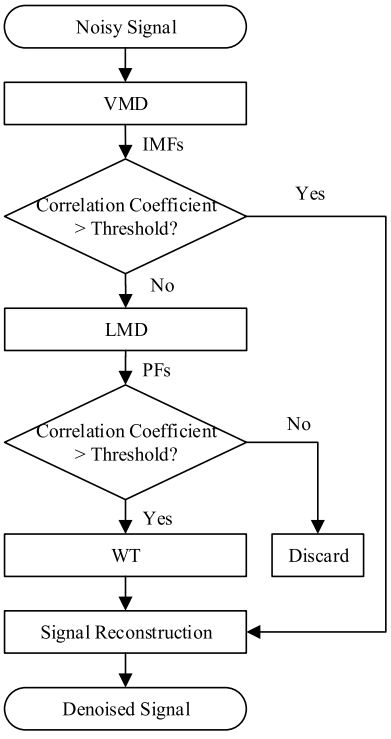

FIGURE 2. Flowchart of the VMD-LMD-WT denoising algorithm.

Figure 2 illustrates the process of the denoising algorithm which involves the following steps:

(1) The VMD is used to divide the noisy radar signals into a sequence of IMFs characterized by different frequency components. This is conducted separately for the I and Q channels of the signals;

(2) To prevent the loss of valid signals resulting from manual selection, the correlation coefficient method is employed to determine the noise-dominated IMFs and signal-dominated IMFs. The following is the definition of the correlation coefficient between IMF and the original radar signal [25]:

$$r_i = \frac{\sum_{j=1}^{n} [x(j) - \overline{x}][y_i(j) - \overline{y_i}]}{\sqrt{\sum_{j=1}^{n} [x(j) - \overline{x}]^2 [y_i(j) - \overline{y_i}]^2}} \tag{12}$$

where r_i is the correlation coefficient between the i-th IMF and the original signal, $i = 1, 2, 3, \cdots, K$, $x(j)$ is the noise-containing signal with sampling point j, $y_i(j)$ is the i component of the decomposed noise-containing signal with sampling point j, $\overline{x}$ represents the mean value of x, and $\overline{y_i}$ means the average of $y(j)$;

(3) Utilize the LMD method to further decompose noise-dominated IMFs selected by thresholding. With the correlation coefficient approach, the decomposed PFs with higher correlation coefficients are reserved, and the others are discarded;

(4) WT denoising method is used to denoise the reserved PFs and remove noise at various frequency bands [26]. The signal-dominated IMFs and the denoised PFs are reconstructed to obtain the denoised signal.

B. NETWORK MODEL

An LPI radar waveform recognition system based on a deep convolutional network is proposed in [27]. The model consists of one convolutional layer, three processing modules, and two fully connected layers, enhancing the performance of LPI radar waveform recognition. In order to achieve multi-scale feature extraction, we present an improved LPI-Net with dilated convolution, which incorporates some modifications from the original LPI-Net. The dilation convolution expands the original 3×3 convolution kernel to 5×5 (dilation rate $=$ 2) or a larger receptive field while keeping the same number of parameters and computational complexity. To prevent information loss, we use variant dilation rates instead of a fixed one. Figure 3 depicts the overall network structure, while Figure 4 depicts the network's inception and processing modules. The main adjustments to the LPI-Net are as follows:

(1) Following the first 7×7 convolutional layer, an inception module is introduced to reduce the dimensionality of the features while enhancing the network's feature extraction capability;

(2) The number of parallel convolutional layers in the processing module is increased to three. Using skip-connections, the concatenate layer collects the learned features from the previous layer to achieve multi-scale and multi-level information fusion;

(3) In the processing module, the convolution kernels are changed from 1×3 and 3×1 to 3×3 and 1×1. Each 3×3 ordinary convolution layer is replaced with a dilated

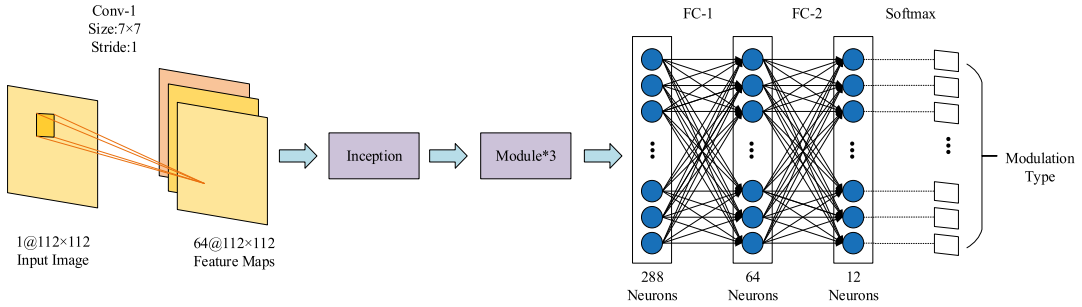

FIGURE 3. The overall structure of the network.

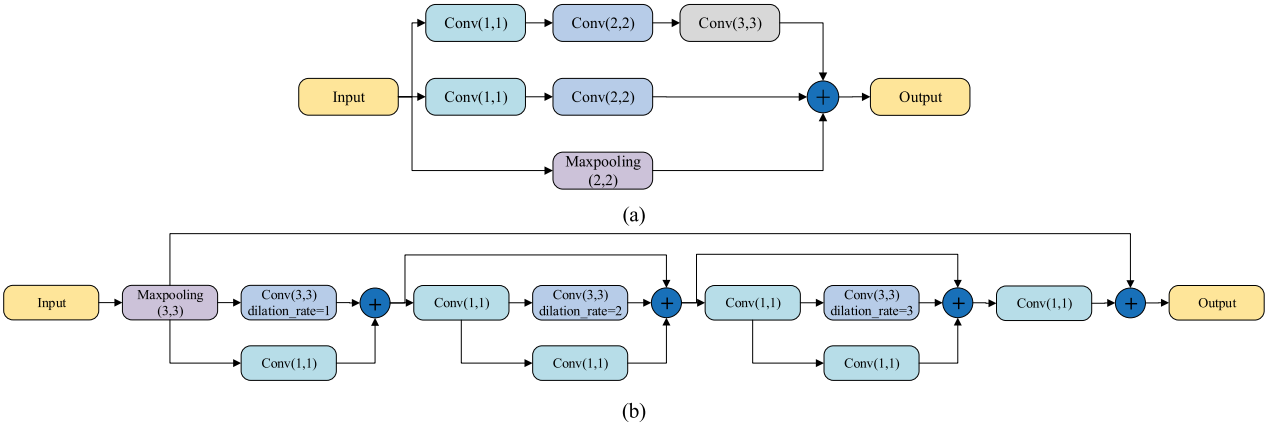

FIGURE 4. The structure of the module. (a) inception module. (b) processing module.

convolution to increase the sensory field without sacrificing the feature map size. And the dilation rate was set to 1, 2, and 4, respectively.

IV. EXPERIMENTS AND DISCUSSION

A. DATASET AND EXPERIMENTAL SETTINGS

In the experiment, the LPI radar signal dataset is created by simulation. The range of SNR is from −14 dB to 10 dB with steps of 2 dB. For each SNR, 400 training samples are created at random for each signal, resulting in a total of 62,400 TFIs. The dataset is split into an 8:2 ratio, with 80% of the samples allocated to the training set and 20% assigned to the validation set. Additionally, 150 test samples of each signal for each SNR are generated to test the training results.

To train the model, we use the cross-entropy function as the loss function and the Adam function as the optimization function. The epoch is set at 100 and the batch size to 64. Every ten epochs, the learning rate is changed from its original value of 0.001 to 0.1 times that value. The experiments are performed on a system equipped with a 2.40GHz CPU and an NVIDIA GeForce RTX 3090 GPU. The models are trained using the Python 3.9.16 programming language and the deep learning model framework TensorFlow 2.12.0. For further research, the code for multilayer decomposition denoising and improved CNN is available at https://github.com/stu-cjlu-sp/rsrc-for-pub/tree/main/VMD-LMD-WT.

B. RESULTS AND ANALYSIS

1) COMPARISON OF DENOISING EFFECT

In the simulation, we take an LFM signal with an SNR of −6 dB as an example. Initially, we conduct a VMD on the radar signal, resulting in nine IMF components spanning from low to high frequencies, as illustrated in Figure 5. The correlation coefficients associated with each IMF component are presented in TABLE 1. It can be seen that the correlation coefficients of IMF_2, IMF_3, and IMF_4 significantly exceed those of the other IMFs. The higher correlation with the original signal implies that these components contain more relevant information. To distinguish between signal-dominant and noise-dominant components, a correlation coefficient threshold of 0.2 is established. Accordingly, IMF_2, IMF_3, and IMF_4 are classified as signal-dominant components and the remaining IMF components are noise-dominant ones.

After that, we extract six PF components from each noise-dominated IMF by using the LMD approach. TABLE 2 lists the correlation coefficients for each PF component after decomposing IMF_1. The correlation coefficient of PF_2 is significantly higher than the others, which indicates that the PF still contains useful information to be further extracted. In contrast, the remaining PFs show lower correlation coefficient and are subsequently eliminated. Based on the above analysis, The correlation coefficient threshold is set to 0.02. Subsequently, the selected PF components undergo

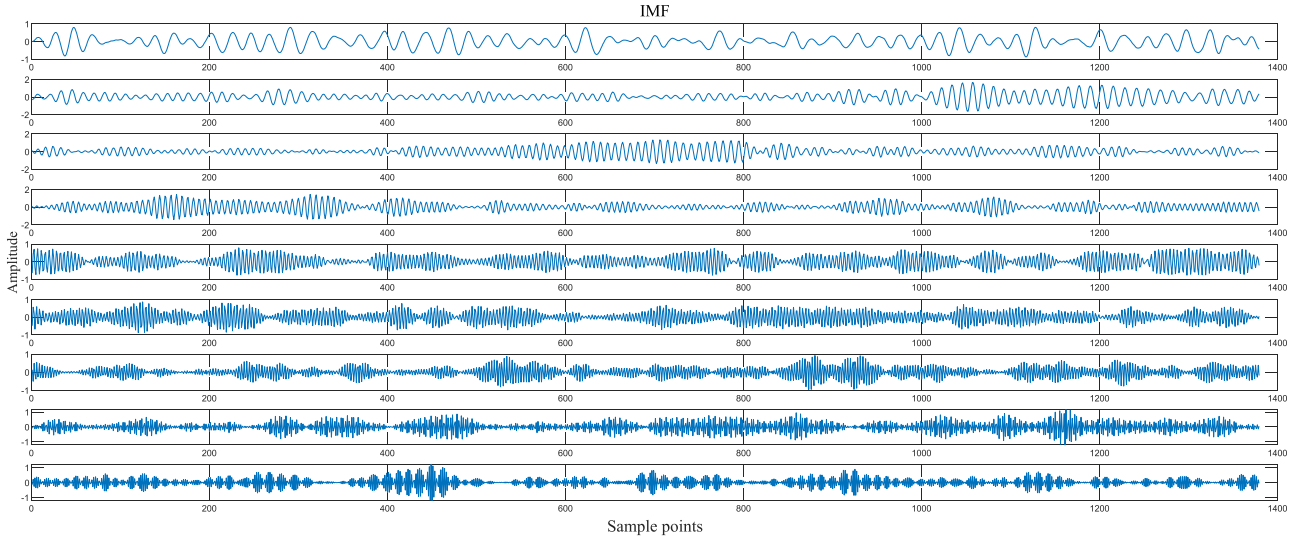

FIGURE 5. VMD decomposition results of LFM signal at SNR = −6 dB.

TABLE 1. Correlation coefficient values for IMF components.

Component	IMF_1	IMF_2	IMF_3	IMF_4	IMF_5	IMF_6	IMF_7	IMF_8	IMF_9
Correlation Coefficient	0.0501	0.4256	0.4699	0.3769	0.0078	0.0031	0.0023	9.6343e-04	7.5388e-04

TABLE 2. Correlation coefficient values for PF components.

Component	PF_1	PF_2	PF_3	PF_4	PF_5	PF_6
Correlation Coefficient	-8.2212e-04	0.0737	0.0039	-0.0063	-6.8710e-04	-0.0015

a denoising process using the WT to extract valuable information from them. After denoising, the PF components are reconstructed only with the signal-dominant components, resulting in the VMD-LMD-WT denoised signal.

To evaluate performance of our suggested denoising approach, we compare it with two commonly used algorithms, ensemble empirical mode decomposition (EEMD) [28] and VMD-WT [29]. In Figure 6, we present the signal waveforms before and after denoising using the three aforementioned algorithms. Figure 6(a) illustrates the waveform before denoising and Figure 6(b-d) show the waveforms after denoising using EEMD, VMD-WT, and VMD-LMD-WT, respectively. It is observed that the noise interference in the signal is significantly reduced by using the VMD-WT and VMD-LMD-WT algorithms, whereas the EEMD shows limitations in reconstruction waveform with residual noise interferences.

The SNR is adopted to further measure the performance of signal denoising, which can be written as:

$$SNR_{out} = 10\lg\left\{\frac{\sum_{i=1}^{N} x(t)^2}{\sum_{i=1}^{N}[x(t)-x'(t)]^2}\right\} \tag{13}$$

where $x(t)$ and $x'(t)$ represent the original input signal and the denoised signal, N indicates the number of sampling points.

TABLE 3. SNR_{out} under different denoising methods.

Denoising algorithms	SNR_{in} / dB				
	-14	***-8***	***-2***	***4***	***10***
EEMD	-11.57	-5.53	0.21	4.23	10.79
VMD-WT	-2.42	-0.24	3.75	8.29	13.03
VMD-LMD-WT	-2.24	0.48	4.77	9.51	14.31

TABLE 3 compares the SNR before and after denoising using three different algorithms. As the input SNR increases, the SNR improvement shows a general decreasing trend. When the SNR is −14 dB, the SNR improvement value reaches the maximum, and the proposed VMD-LMD-WT can improve the SNR by about 11.76 dB, which outperforms the other two denoising methods. In general, the VMD-LMD-WT algorithm is highly effective in filtering out the

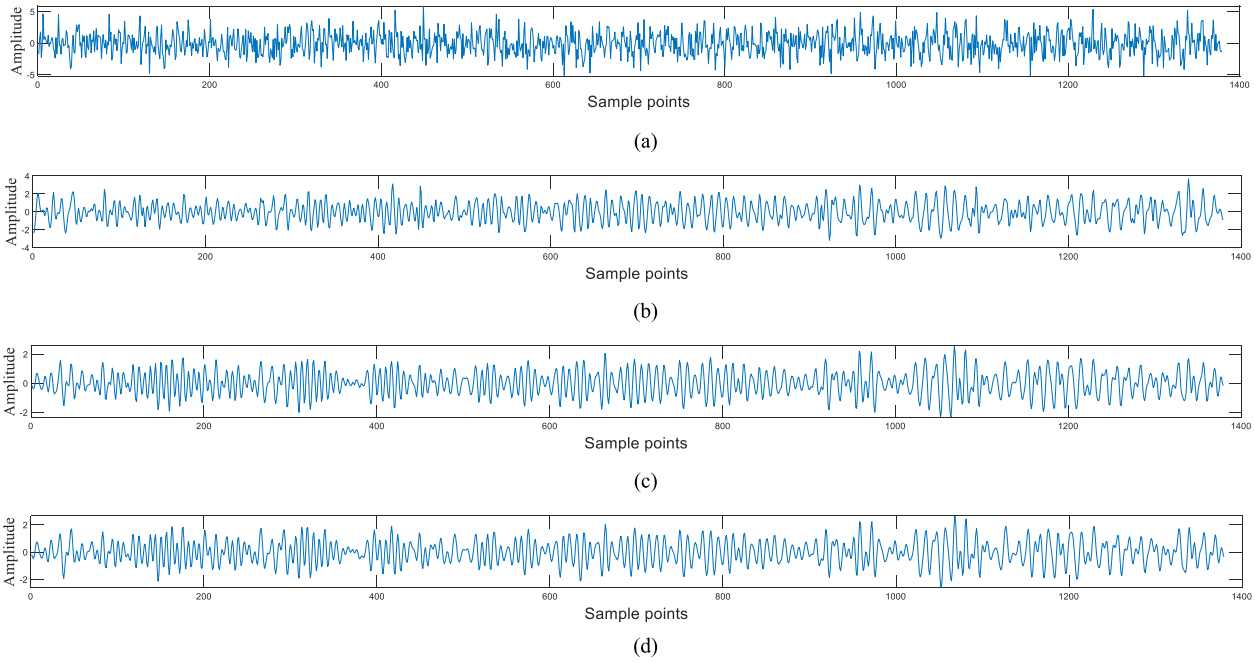

FIGURE 6. Noisy and denoised waveforms using three denoising algorithms. (a) noisy signal. (b) denoised signal by EEMD. (c) VMD-WT. (d) VMD-LMD-WT.

Gaussian noise from the LPI radar signal to emphasize its signal characteristics.

2) EFFECTIVENESS OF MULTILAYER DENOISING ALGORITHM

To assess the effectiveness of the multilayer denoising method, we compare it with EEMD and VMD-WT. For fairness, the neural network is fixed as the proposed CNN model. Figure 7 displays the CWD-TFIs of the noised signal and the denoised signals by three denoising algorithms. Compared to Figure 7(a)(b), Figure 7(c)(d) contain less noise and are visually clearer. Based on this observation, we can conclude that the VMD-WT and VMD-LMD-WT denoising methods are significantly better than EEMD.

Then, we analyze the detection accuracy of 12 signals using the EEMD, VMD-WT, and VMD-LMD-WT denoising algorithm. The results, as shown in Figure 8, indicate that VMD-LMD-WT denoising can achieve a recognition accuracy of 75.3% when the SNR is −14dB. This represents an improvement of approximately 11% compared to the original signal. Additionally, there is also an improvement when compared to the two methods of EEMD and VMD-WT.

Due to the poor performance of EEMD denoising in previous experiments, we further investigate the VMD-WT and VMD-LMD-WT denoising algorithms. We compare the recognition accuracies of these two methods for different radar signals in Figure 9, which demonstrates that the VMD-LMD-WT method has significantly higher recognition accuracy than the VMD-WT method for polyphase codes, especially at low SNR. The foregoing phenomena can be linked to the VMD's poor noise tolerance in high-noise

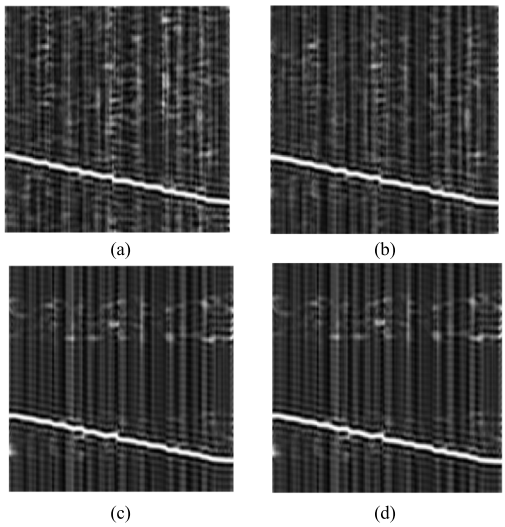

FIGURE 7. CWD-TFIs of the noised signal and the denoised signals by three denoising algorithms. (a) signals with noise. (b) EEMD. (c) VMD-WT. (d) VMD-LMD-WT.

environments. However, in the VMD-LMD-WT method, the VMD and LMD use different signal decomposition strategies, which help to preserve the structural information of multiphase codes more successfully. Additionally, wavelet thresholding provides enough information to handle residual noise more precisely.

Furthermore, we analyze the recognition confusion of the VMD-LMD-WT method. Figure 10 demonstrates that while most signals have higher classification accuracy at SNRs of −10 dB, P1 and P4 codes are still poorly recognized. In fact,

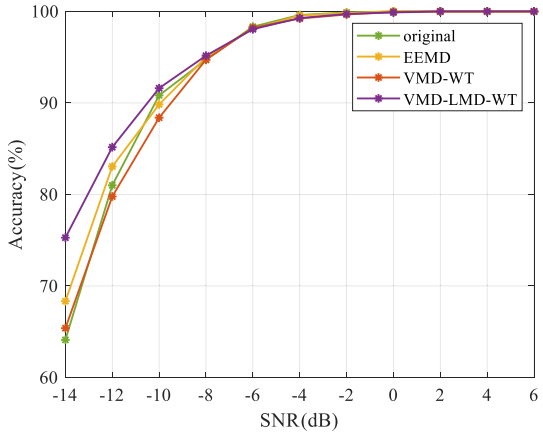

FIGURE 8. Recognition accuracy under different denoising algorithms.

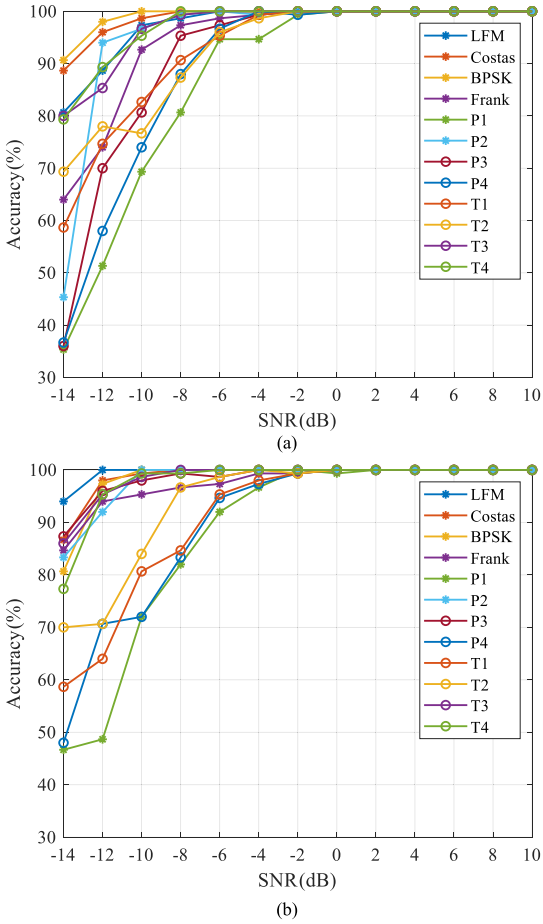

FIGURE 9. Recognition accuracy of different radar signals: (a) VMD-WT; (b) VMD-LMD-WT.

approximately 27% of P1 codes are incorrectly recognized as P4 codes. This is mainly caused by the high bandwidth occupancy and frequency jitter of polyphase codes in both the time and frequency domains. When dealing with such high-dynamic-range and fast-transforming signals, the VMD and LMD may not be able to capture the details and features of the signals, resulting in poor denoising results.

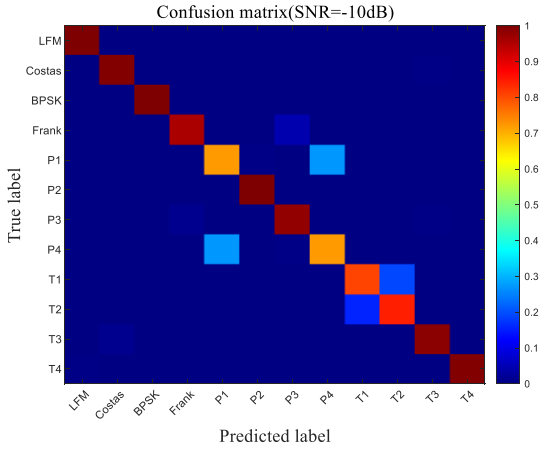

FIGURE 10. Confusion matrix for SNR = −10dB.

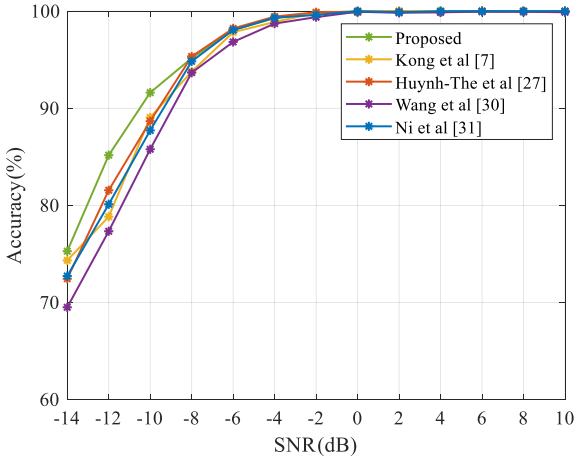

FIGURE 11. Accuracy of different neural networks.

3) PERFORMANCE COMPARISON OF DIFFERENT MODELS

In this section, experiments based on different neural networks are conducted to validate the superiority of our proposed network. The input data is the TFI of the signal denoised using the VMD-LMD-WT denoising technique. We compare the proposed model with other models, proposed by Kong et al. [7], Huynh-The et al. [27], Wang et al. [30], and Ni et al. [31]. The comparison results are shown in Figure 11. Figure 11 demonstrates that our model achieves the highest accuracy at almost every SNR level. When the SNR increases to 0 dB, the classification accuracies of all compared algorithms approach 100%. At an SNR of −12dB, our model has a classification accuracy of 85.17%, which is approximately 6% and 3% better than the CNN suggested by Kong et al. and Huynh-The et al., respectively. We attribute this improvement to the introduction of dilated convolutions and the modifications of network structure. Dilated convolutions increase the receptive field by introducing blank space in the convolutional kernel. In the low SNR environment, dilated convolution has the better ability to capture of contextual information as compared with the conventional counterpart, enhancing the

ability of model to understand and accurately recognize signals. The increase in skip connections enables the direct connection of information from lower levels to higher levels, facilitating better integration of features from different levels of the network. This improvement contributes to the overall performance of the model.

V. CONCLUSION

In this paper, a novel method is proposed for radar signal recognition under low SNR scenarios by leveraging a multilayer denoising scheme and improved CNN. The multilayer denoising algorithms and neural network adjustments are the two key measures that contribute to the success of the proposed method. The proposed method uses a combination of VMD, LMD, and WT for effective multi-layer noise reduction. In comparison to existing denoising methods, the proposed multilayer denoising approach demonstrates the capability to enhance the SNR significantly. The introduction of this denoising method can potentially improve the quality of TFIs, thereby contributing to improved identification performance. In addition, the recognition network incorporates dilated convolution to increase the sensing field without increasing the number of parameters. Simulation results demonstrate that the proposed method achieves a recognition accuracy of 75.3% for 12 radar modulation signals when the SNR is as low as -14 dB. In future work, we will focus on the study of the sophisticated signal decomposition methods to enhance the denoising effect of TFIs, and the design of network architecture to improve the recognition accuracy of the radar signals.

REFERENCES

[1] Z. Zhou, G. Huang, and H. Chen, "An overview of radar emitter recognition algorithms," *Telecommun. Eng.*, vol. 57, no. 8, pp. 973–980, 2017.

[2] Z. Hu, J. Huang, D. Hu, and Z. Wang, "A time-frequency image denoising method via neural networks for radar waveform recognition," *IEEE Commun. Lett.*, vol. 27, no. 1, pp. 150–154, Jan. 2023.

[3] Z.-L. Wu, X.-X. Huang, M. Du, X.-S. Xu, D. Bi, and J.-F. Pan, "Intrapulse recognition of radar signals via bicubic interpolation WVD," *IEEE Trans. Aerosp. Electron. Syst.*, vol. 59, no. 6, pp. 8668–8680, Dec. 2023.

[4] X. Zhang, L. Zuo, D. Yang, and J. Guo, "Coherent-like integration for PD radar target detection based on short-time Fourier transform," *IET Radar, Sonar Navigat.*, vol. 14, no. 1, pp. 156–166, Jan. 2020.

[5] M. Zhang, M. Diao, and L. Guo, "Convolutional neural networks for automatic cognitive radio waveform recognition," *IEEE Access*, vol. 5, pp. 11074–11082, 2017.

[6] Z. Qu, C. Hou, C. Hou, and W. Wang, "Radar signal intra-pulse modulation recognition based on convolutional neural network and deep Q-learning network," *IEEE Access*, vol. 8, pp. 49125–49136, 2020.

[7] S.-H. Kong, M. Kim, L. M. Hoang, and E. Kim, "Automatic LPI radar waveform recognition using CNN," *IEEE Access*, vol. 6, pp. 4207–4219, 2018.

[8] L. M. Hoang, M. Kim, and S.-H. Kong, "Automatic recognition of general LPI radar waveform using SSD and supplementary classifier," *IEEE Trans. Signal Process.*, vol. 67, no. 13, pp. 3516–3530, Jul. 2019.

[9] J. Yu and J. Lv, "Weak fault feature extraction of rolling bearings using local mean decomposition-based multilayer hybrid denoising," *IEEE Trans. Instrum. Meas.*, vol. 66, no. 12, pp. 3148–3159, Dec. 2017.

[10] N. E. Huang, Z. Shen, S. R. Long, M. C. Wu, H. H. Shih, Q. Zheng, N.-C. Yen, C. C. Tung, and H. H. Liu, "The empirical mode decomposition and the Hilbert spectrum for nonlinear and non-stationary time series analysis," *Proc. Roy. Soc. London. Ser. A, Math. Phys. Eng. Sci.*, vol. 454, no. 1971, pp. 903–995, Mar. 1998.

[11] M. Han, Y. Wu, Y. Wang, and W. Liu, "Roller bearing fault diagnosis based on LMD and multi-scale symbolic dynamic information entropy," *J. Mech. Sci. Technol.*, vol. 35, no. 5, pp. 1993–2005, May 2021.

[12] K. Dragomiretskiy and D. Zosso, "Variational mode decomposition," *IEEE Trans. Signal Process.*, vol. 62, no. 3, pp. 531–544, Feb. 2014.

[13] Y. Li, C. Zhang, and Y. Zhou, "A novel denoising method for ship-radiated noise," *J. Mar. Sci. Eng.*, vol. 11, no. 9, p. 1730, Sep. 2023.

[14] Y. Li, B. Tang, and S. Jiao, "SO-slope entropy coupled with SVMD: A novel adaptive feature extraction method for ship-radiated noise," *Ocean Eng.*, vol. 280, Jul. 2023, Art. no. 114677.

[15] J. Ma, J. Wu, and X. Wang, "Incipient fault feature extraction of rolling bearings based on the MVMD and teager energy operator," *ISA Trans.*, vol. 80, pp. 297–311, Sep. 2018.

[16] Y. Li, B. Tang, and Y. Yi, "A novel complexity-based mode feature representation for feature extraction of ship-radiated noise using VMD and slope entropy," *Appl. Acoust.*, vol. 196, Jul. 2022, Art. no. 108899.

[17] Z. Jiang, J. Xie, J. Zhang, and X. Zhang, "Denoising method of pipeline leakage signal based on VMD and Hilbert transform," *J. Sensors*, vol. 2023, pp. 1–16, Feb. 2023.

[18] C. Zhang, Z. Zhou, and S. Zhou, "SEMG signal denoising based on variational mode decomposition and wavelet thresholding," in *Proc. 5th Int. Conf. Intell. Control, Meas. Signal Process. (ICMSP)*, Chengdu, China, May 2023, pp. 913–916.

[19] Q. Zhai, M. Zhu, Y. Li, and Y. Li, "Recognition of overlapped radar signals via VMD-based multi-label learning," in *Proc. IET Int. Radar Conf.*, vol. 2020, Nov. 2020, pp. 133–137.

[20] X. Wei, G. Feng, T. Qi, J. Guo, Z. Li, D. Zhao, and Z. Li, "Reduce the noise of transient electromagnetic signal based on the method of SMA-VMD-WTD," *IEEE Sensors J.*, vol. 22, no. 15, pp. 14959–14969, Aug. 2022.

[21] W. Ding, S. Hou, S. Tian, S. Liang, and D. Liu, "A Bayesian optimized variational mode decomposition-based denoising method for measurement while drilling signal of down-the-hole drilling," *IEEE Trans. Instrum. Meas.*, vol. 72, pp. 1–14, 2023.

[22] J. Yu and Z. Zhang, "Research on the seismic signal denoising with the LMD and EMD method," in *Proc. IEEE 2nd Adv. Inf. Technol., Electron. Autom. Control Conf. (IAEAC)*, Mar. 2017, pp. 767–771.

[23] J. S. Smith, "The local mean decomposition and its application to EEG perception data," *J. Roy. Soc. Interface*, vol. 2, no. 5, pp. 443–454, Dec. 2005.

[24] S. Yue, Y. Wang, L. Wei, Z. Zhang, and H. Wang, "The joint empirical mode decomposition-local mean decomposition method and its application to time series of compressor stall process," *Aerosp. Sci. Technol.*, vol. 105, Oct. 2020, Art. no. 105969.

[25] C. Li, Y. Wu, H. Lin, J. Li, F. Zhang, and Y. Yang, "ECG denoising method based on an improved VMD algorithm," *IEEE Sensors J.*, vol. 22, no. 23, pp. 22725–22733, Dec. 2022.

[26] H. Li, J. Shi, L. Li, X. Tuo, K. Qu, and W. Rong, "Novel wavelet threshold denoising method to highlight the first break of noisy microseismic recordings," *IEEE Trans. Geosci. Remote Sens.*, vol. 60, 2022, Art. no. 3142089.

[27] T. Huynh-The, V.-S. Doan, C.-H. Hua, Q.-V. Pham, T.-V. Nguyen, and D.-S. Kim, "Accurate LPI radar waveform recognition with CWD-TFA for deep convolutional network," *IEEE Wireless Commun. Lett.*, vol. 10, no. 8, pp. 1638–1642, Aug. 2021.

[28] Z. Wu and N. E. Huang, "Ensemble empirical mode decomposition: A noise-assisted data analysis method," *Adv. Adapt. Data Anal.*, vol. 1, no. 1, pp. 1–41, Jan. 2009.

[29] T. Qi, X. Wei, G. Feng, F. Zhang, D. Zhao, and J. Guo, "A method for reducing transient electromagnetic noise: Combination of variational mode decomposition and wavelet denoising algorithm," *Measurement*, vol. 198, Jul. 2022, Art. no. 111420.

[30] C. Wang, J. Wang, and X. Zhang, "Automatic radar waveform recognition based on time-frequency analysis and convolutional neural network," in *Proc. IEEE Int. Conf. Acoust., Speech Signal Process. (ICASSP)*, New Orleans, LA, USA, Mar. 2017, pp. 2437–2441.

[31] X. Ni, H. Wang, Y. Yang, Y. Zhu, and Z. Zhang, "Polyphase-modulated radar signal recognition based on time-frequency amplitude and phase features," in *Proc. 13th Int. Congr. Image Signal Process., Biomed. Eng. Informat. (CISP-BMEI)*, Chengdu, China, Oct. 2020, pp. 552–556.

MENGTING JIANG received the B.S. degree in communications engineering from China Jiliang University, Hangzhou, China, in 2022, where she is currently pursuing the M.S. degree. Her research interests include radar signal recognition and modulation classification.

FANG ZHOU received the B.S., M.S., and Ph.D. degrees in electronics engineering from Xidian University, Xi'an, China, in 2006, 2009, and 2018, respectively. From 2011 to 2022, she was a Researcher with the Guilin University of Electronic and Technology. Since 2023, she has been an Associate Professor with China Jiliang University. Her research interests include filter bank design, graph signal processing, and signal recognition.

LAI SHEN received the B.S. degree in electronic science and technology from Anhui University of Science and Technology, Bengbu, China, in 2020. He is currently pursuing the M.S. degree with China Jiliang University, Hangzhou, China. His research interests include radar signal recognition and modulation classification.

XIAOFENG WANG received the M.S. degree in communication and information systems from Yunnan University, Kunming, China, in 2012, and the Ph.D. degree in information and communication engineering from Shanghai Jiao Tong University, Shanghai, China, in 2017. He is currently a Lecturer with the School of Information Engineering, China Jiliang University, Hangzhou, China. His research interests include network science, data mining, artificial intelligence, and machine learning.

DAYING QUAN (Member, IEEE) received the B.S. degree in automatic control and the M.S. degree in information and communication engineering from Xi'dian University, Xi'an, China, in 2001 and 2004, respectively. He was with Hangzhou Silan Microelectronics Company Ltd. (2004–2008). Then, he was with Eastern Communications Company Ltd., and had been working on professional communication systems (2009–2014). In 2014, he joined China Jiliang University and is currently working on wireless signal processing and intelligent wireless sensing.

NING JIN received the B.S. and master's degrees in information and electronic engineering from Zhejiang University, Hangzhou, Zhejiang, China, in 1988 and 1991, respectively. She is currently a Professor with the Information Engineering College, China Jiliang University. Her research interests include intelligent systems, wireless networks, and signal processing.